Please cite the Published Version

Data Access Statement: The manuscript contains all data supporting the reported results.

Title:

Structural adaptations of the beak and oropharyngeal cavity roof in migratory *Anas crecca*: distinctive scanning electron microscopic pattern of its filter feeding apparatus

Authors and affiliations:

Reem S. Alruhaimi[1], Mohamed M. A. Abumandour[2]*, Mohammed Kassab[3], Ahmed A. Elnegiry[4], Foad Farrag[5,6], Diaa Massoud[7,8], Ayman M. Mahmoud[9,10]*, Hazem Hamoda[11]

[1]Department of Biology, College of Science, Princess Nourah bint Abdulrahman University, Riyadh 11671, Saudi Arabia.

[2]Department of Anatomy and Embryology, Faculty of Veterinary Medicine, Alexandria University, Alexandria, Egypt.

[3]Department of Cytology and Histology, Faculty of Veterinary Medicine, Kafrelsheikh University, Kafrelsheikh, Egypt.

[4]Department of Histology and Cytology, Faculty of Veterinary Medicine, Aswan University, Aswan, Egypt.

[5]Department of Anatomy and Embryology, Faculty of Veterinary Medicine, Kafrelsheikh University, 33511 Kafrelsheikh, Egypt.

[6]Department of Basic veterinary sciences, Faculty of Veterinary Medicine, Delta University for Science and Technology, Dakahlia, Egypt.

[7]Department of Biology, College of Science, Jouf University, Sakaka, Saudi Arabia.

[8]Department of Zoology, Faculty of Science, Fayoum University, Fayoum, Egypt.

[9]Department of Life Sciences, Faculty of Science and Engineering, Manchester Metropolitan University, Manchester, UK.

[10]Physiology Division, Department of Zoology, Faculty of Science, Beni-Suef University, Beni-Suef, Egypt.

[11]Department of Anatomy and Embryology, Faculty of Veterinary Medicine, Aswan University, Aswan, Egypt.

Correspondence:

Mohamed Abumandour, PhD

Anatomy & Embryology Department, Faculty of Veterinary Medicine, Alexandria University, Egypt. E-mail: M.abumandour@alexu.edu.eg

Ayman M. Mahmoud, PhD

Department of Life Sciences, Faculty of Science and Engineering, Manchester Metropolitan University, Manchester M1 5GD, UK. E-mail: a.mahmoud@mmu.ac.uk

ORCID ID: 0000-0003-0279-6500

ABSTRACT

There is insufficient data about the migratory duck *Anas crecca,* especially the beak and oropharyngeal cavity roof. This study aimed to characterize the beak and palatine adaptations and relate the morphological features with the species-specific feeding behavior of *Anas crecca* collected near Lake Nasser (Egypt). Our study was carried out with the help of gross, scanning electron microscopy (SEM), and morphometric analysis. The lower median papillary teeth-like region corresponded to the lower papillary region in terms of food particle capture. The serrated gnathotheca surface exhibited transverse, wedge-like, cap-like, and serrated border-like processes. The lower mandibular space had four spaces: the rostral smooth, the middle folded, the long sublingual, and the caudal sublaryngeal space. The palate showed two major regions, the rostral long beak (beak nail, middle part, and the caudal papillary part) and the connecting region. The choana consists of the rostral narrow part, which has rostral non-papillated and caudal papillated parts, and the caudal papillated wide part, which has three papillary rows. The infundibular plate had numerous small papillae and sphenopterygoid salivary gland openings. Functionally, the beak plays an important role in the sieving filter feeding mechanism, and the palate is involved in the fixation of the captured food particles inside the oral cavity. Consequently, beak and palate structures exhibit anatomical adaptations for efficiently filtering feeding mechanisms.

Key words: *Anas crecca*; beak; Choana; Infundibulum; Palatine papillae.

1. INTRODUCTION

Anas crecca, also known as the Eurasian teal, common teal, or Eurasian green-winged teal, is a widespread and common migratory waterbird duck that breeds throughout Asia and Europe before migrating to the Mediterranean shores during the winter season. The entire Nile Valley, in particular Lake Nasser, is another significant wintering destination (BirdLife International,

2020). The *Anas* genus belongs to the *Anatidae* family. The Agreement on the Conservation of African-Eurasian Migratory Waterfowl (AEWA) includes *A. crecca* as one of the species. During the spring and summer, mollusks, worms, insects, and crabs are the main food sources. In rare instances, *A. crecca* may dive for prey while submerging its head. However, *A. crecca* generally consumes via dabbling, upending, or grazing. During the breeding (nesting) period, it primarily eats aquatic invertebrates, including crustaceans, insects and their larvae, mollusks, and worms (Madge and Burn, 1988). In the winter, it shifts to a predominantly granivorous habit, eating the seeds of grasses and aquatic plants, such as sedges and grains. Although having nocturnal habits in the winter, diurnal feeding habits exist during the breeding season.

Ingestion, intra-oral transport, and swallowing represent the typical three phases of the feeding process in vertebrates (Schwenk and Rubega, 2005). The behavioral analysis of the feeding process identified evolutionary differences between the neognathous and paleognathous bird groups (Tomlinson, 2000). Food is carried directly into the esophagus without utilizing the tongue in the catch-and-throw dietary habit of paleognathous birds, which is referred to as a cranioinertial mechanism. The intricate movements of the beak and hyolingual apparatus are connected to the lingual feeding mechanism used by neognathous birds. Neognathous birds occasionally use a catch-and-throw system, although it is only employed when swallowing large food particles and still necessitates intricate movements of the hyolingual apparatus. Toucans, hornbills, and southern cassowaries are the outliers among neognathous birds because they develop what is known as ballistic transport (Baussart and Bels, 2011; Bels and Baussart, 2006). Wild ducks have maintained the ability to pick up and toss grains smaller than a pea, as well as removing grass blades (Kooloos et al., 1989). These wild ducks typically eat food that is submerged in water using the filter-feeding strategy (Abumandour et al., 2019; Kooloos et al., 1989; Tomlinson, 2000). Filtration shows typical neognathous bird behaviors such as duck that use lingual feeding and under-tongue conveyance (Kooloos et al., 1989; Tomlinson, 2000).

Most of the published articles only focused on the anatomical description of the tongue of the avian species belonging to the *Anatidae* family and its papillary system and how it adapts to feeding behavior and the availability of food sources (Abumandour and Kandyel, 2020; Jackowiak et al., 2011), while they completely neglected the main role of the beak and the palate in the achievement of the filter-feeding strategy.

The horny upper and lower beaks of birds demarcate their oral cavities, which contain numerous structures related to the specific feeding pattern of each avian species, such as the tongue, laryngeal entrance on the floor, and incomplete palate and infundibular area on the roof (Nickel et al., 1977). Because the former cavities don't have a soft palate like those found in mammals, they are referred to as oropharynxes (King and McLelland, 1984). Recently, it has piqued the curiosity of numerous authors to describe the oropharyngeal cavities of various avian species (Bassuoni et al., 2022; El-Mansi et al., 2021; Gewaily and Abumandour, 2020). Most of the published data have focused on the structural adaptations of the tongue and its vital role on the feeding mechanism (Abumandour and Kandyel, 2020; Jackowiak et al., 2011), with little attention paid to the role of the beak and palate in feeding behaviors, including food particle intakes. Recently, anatomical articles have been directed to study the avian's oropharyngeal cavity structures, including the palate and beak, as well as their modifications to feeding techniques (Abumandour and El-Bakary, 2017; Abumandour and Gewaily, 2018, 2019; Bassuoni et al., 2022; El-Mansi et al., 2020; El-Mansi et al., 2021; Gewaily and Abumandour, 2020; Tadjalli et al., 2008). However, there are very few anatomical details about the oropharyngeal cavities of the different duck species, especially the migratory species. There is scanty information about the morphological characterizations of the oropharyngeal cavity roof with its palate and infundibular area and their role in the feeding mechanism, including the food particle intakes. As a result, we used gross and scanning electron microscopic (SEM) examinations to describe the structural adaptations of the beak, the incomplete palate, and the

infundibular area and their role in the feeding filtering apparatus of the migratory duck (*A. crecca*) collected around Lake Nasser (Aswan, Egypt).

2. MATERIALS AND METHODS

2.1. Collection of samples and gross anatomical examination

This study was carried out according to the Institutional Animal Care and Use Committee (IACUC) protocols of Laboratory Animals, Faculty of Veterinary Medicine, Alexandria University (Approval no.: 11/3/2023/232). Ten *A. crecca* duck were obtained from a local hunter near Lake Nasser in Aswan (Egypt). The collected ducks were kept in the animal housing following the guidelines established for the 'Sampling protocol for the pilot collection of catch, effort, and biological data in Egypt' (Dimech et al., 2012). The ducks included in the study were free from any oropharyngeal anatomical abnormalities. The ducks were anesthetized with pentobarbitone sodium administered through the internal carotid artery with warm physiological saline (35 °C). The oropharyngeal cavity roof (incomplete palate and infundibular area) and beak, as well as the lower and upper mandibular rami comprising the beak, obtained by dissecting the heads longitudinally (n = 5), were photographed on five samples using a digital camera (Cannon IXY 325, Japan).

2.2. SEM examination

To investigate the ultrastructural features five samples were fixed at 4°C in 2% formaldehyde, 1.25% glutaraldehyde in a 0.1 M sodium cacodylate buffer (pH 7.2). The samples were washed in 0.1 M sodium cacodylate containing 5% sucrose, processed through tannic acid, and finally dehydrated in increasing concentrations of ethanol (50, 70, 80, 90, 95, and 100% ethanol, 15 min each). After critical point drying in carbon dioxide, the samples were attached to stubs with colloidal carbon and coated with gold palladium in a sputtering device. Specimens were examined and photographed with a JEOL SEM operating at 15 KV at the Faculty of Science,

Alexandria University, Egypt. The characteristic features of the obtained images were colored by the Photo Filter 6.3.2 program to realize the diverse structures according to Roshdy et al (2021).

2.3. Morphometric and statistics analyses

The dimensions of the incomplete palate, choanal cleft with its rostral and caudal part, infundibular area, and the lower and upper mandibular rami forming the beak were measured using an electronic ruler with an accuracy of 0.1 mm and a camera (IXY 325, Canon, Japan). The obtained data were expressed as mean ± standard deviation values and statistically evaluated using student's t-test to compare the means.

3. RESULTS

3.1. The lower beak

3.1.1. Gross morphometric analysis

The oropharyngeal cavity floor consists of the free rostral, the lingual, and the laryngeal regions. The free rostral region represented 9%, the lingual region represented 63.6%, and the laryngeal region represents 27.2% of the oropharyngeal cavity floor length (Table 1). The oropharyngeal cavity floor was formed from the elongated lower mandible that had two lateral elongated lower rami that enclosed an elongated lower mandibular space that was divided into free rostral, lingual, and laryngeal regions. The length of lower mandibular space till beginning of lingual frenulum represented 76%, the length of the rostral smooth space 4%, the length of the middle folded space 6%, the length of the middle folded space 80%, and the length of the caudal sublaryngeal space 10% of the length of the lower mandibular space (Table 1).

3.1.2. Gross observations

Grossly, the oropharyngeal cavity floor was formed of the elongated lower mandible, which was bounded laterally by a hard keratinized structure called gnathotheca. The lower mandible

has two surfaces, the smooth internal surface and the serrated external surface of the keratinized gnathotheca (Figs. 1-4A, 1B/GT). The lower mandible showed two lateral elongated lower mandibular rami that communicated rostrally through the semilunar rostrally convex part of the gnathotheca (Figs. 1A, 2A-B, and 4A/LRB, RPB).

These two rami enclosed the elongated lower mandibular structure that was divided into free rostral, lingual, and laryngeal regions. The free rostral region has two portions, the rostral short smooth space and middle short folded space. The lingual region has the sublingual space that enclosed an elongated tongue fixed to this space floor by the lingual frenulum, and the laryngeal region has the elevated laryngeal entrance (Figs. 1A, 2A-B, 4A, 5A/SDR, FDR, SLS, TO, LF, and PR).

3.1.3. SEM observations

The semilunar teeth-like papillary region was bordered rostrally by the rostral semilunar convex border of the keratinized part of the gnathotheca and caudally by the elevated internal beak ridge, which carried numerous beak scales (Figs. 1B-C, 3A/TPR, RPB, IBR, SB). Each teeth-like papilla of the median region had a serrated apex and round base that originated from a rounded-like depressed space that was bordered by a circular border of 2-3 circular layers (Fig. 1C-D, 1G-F/TPR, TP, white and black arrowheads), while those located at the periphery of this teeth-like papillary region were triangular with an oblique rostrally direction in which each was surrounded by a shallow space and an incomplete caudal border (Fig. 1G-F/TP, white and black arrowheads). At the median teeth-like papillary region, there are numerous filiform-like papillae between a circular border surrounding each teeth-like papilla (Fig. 1C-D/BF), but they are completely absent at the peripheral part of this region.

The externally serrated surface of the keratinized gnathotheca was separated from the mandible ramus by a shallow longitudinal groove (Fig. 1B, 1E, 1H, 2C-D, 3A, 4B-C/LRB, SLR, red asterisk) and from the rostral semilunar convex border of the keratinized part of the gnathotheca

by an oblique shallow groove (Fig. 1B/RPB, LRB, RBG). This serrated border had three regions. The first short region extended for 0.4 cm and was located opposite the rostral part of the free rostral region of the lower mandibular space, just caudal to the level of the junction with the rostral semilunar convex border of the keratinized part of the gnathotheca. It showed slightly oblique long transverse processes separated by a shallow groove and a wedged-like projected process (Fig. 1B, 1E, 1H, 2C, 3A/SLR, VP, red arrowheads, WP). The second short region was located opposite to the caudal part of the free rostral region of the lower mandibular space just caudal to the first region and extended for 0.5 cm and possessed slightly oblique long transverse processes that separated from each other by a shallow groove and a convex externally cap-like processes (Fig. 2D-E/SLR, VP, red arrowheads, CP). The third long region was located opposite the lingual region of the lower mandibular space to the level of the lingual root and possesses slightly oblique long transverse processes that were separated from each other by a shallow groove and the serrated border-like processes (Fig. 2F, 4B-C, 5B-G, 6/SLR, VP, red arrowheads, BSP). Each characteristic serrated border-like process appeared to originate from the apex of the slightly oblique long transverse process and be separated from each other by inter-process space that possessed an irregular surface with numerous scales (Fig. 2F, 4B-C, 5B-G, 6/BSP, IPS). From the level of the rostral border of the lingual frenulum, each serrated border-like process is composed of separated triangular pointed processes with a small space between them (Fig. 6/BSP, IPS). With magnification, there were numerous scales at the smooth beak space and between the processes of the lateral serrated border of the beak ramus (Fig. 3A, 5D, and 5G/BS).

The elongated lower mandibular space between the two beak rami was subdivided into three spaces, free rostral short smooth, middle short folded, and the long deep sublingual, and the caudal sublaryngeal space that was completely fixed and attached to the laryngeal mound (Fig. 2A-B, 4A, 5A, 7A-D/SDR, FDR, LRB, LF). The ovoid rostral short smooth space was located

between the teeth-like papillary region rostrally and the semilunar transverse palatine fold (Fig. 1B, 1E, 1H, 3A/SDR, FDR, SLS, LF). The middle short folded space contained numerous scales and two types of the salivary gland openings; two circular large maxillary salivary gland openings were partially covered by the keratinized skin and located just caudal to the lateral border of the semilunar transverse palatine fold and numerous small palatine salivary gland openings just caudal to the central of the semilunar transverse palatine fold (Fig. 1B, 3/FDR, TPF, BS, blue and green arrowheads, KS). The long deep sublingual space enclosed an elongated tongue, which was fixed to the floor of the oropharyngeal cavity by an elongated tongue-like lingual frenulum at its caudal part, just at the level of the lingual prominence. On each side of the shallow elevated median ridge (at the middle part of the sublingual space just at the level of the rostral part of the lingual body), there are two types of palatine salivary gland openings; two large ovoid openings and numerous small round openings (Fig. 4/SLS, LF, MSR, red and green arrowheads, KS). On each side of the shallow elevated median ridge (just rostral to the lingual frenulum), there are numerous oblique folds, but under the lingual frenulum there are sublingual muscles (Fig. 5B, 5E, 6A-B/SLS, LF, MSR, SLF, and SLM).

3.1.4. SEM morphometric analysis of the different beak processes

The longest beak processes are the serrated border-like processes then the transverse processes while the wedge-like processes are the shortest ones (Table 2). The widest ones are the cap-like processes then the transverse processes while the less ones are wedge-like processes (Table 2).

3.2. Oropharyngeal cavity roof with its upper beak

3.2.1. Gross morphometric analysis

The upper mandible incomplete palate was divided into rostral long beak (that subdivided into the rostral ridged part, including the beak nail; the middle smooth part; and the caudal papillary

part), and the caudal connecting region (that subdivided into the choanal and infundibular region). The rostral long beak represented about 54% and the caudal connecting region represented about 46% of the oropharyngeal cavity roof length (Table 3). The rostral ridged part represented about 10%, the beak nail represented about 4%, the middle smooth part represented about 56%, and the caudal papillary part represented about 30% of the length of the rostral long beak part (Table 3). The choanal region represented about 26% and the infundibular region represented about 11% of the oropharyngeal cavity roof length (Table 3), while the rostral narrow choanal part was represented about 26% and the caudal papillated wide choanal part represented about 74% of the choanal length (Table 3). The length of the median palatine ridge represented 52%, the length of the median palatine papillary ridge represented 22%, the length of the paramedian palatine papillary ridge represented 19%, and the length of each transverse palatine ridge represented 7% (Table 3).

3.2.2. Gross observations

The incomplete palate made up the oropharyngeal cavity's roof, which was bordered externally by the hard, keratinized, externally serrated, nearly straight lower beak (Fig. 3A, 4A, 7A-B, 9A, 10A, 11A, 12A, 13A-B). The oropharyngeal cavity roof was formed of the elongated upper mandible, which was bounded laterally by a hard keratinized structure called the rhinothecae. The upper mandible showed smooth external surface and the ridged inner surface of the keratinized rhinothecae (Figs. 7, 8A-B, 10A/RT). The upper mandible had two lateral elongated upper mandibular rami that communicated rostrally by the semilunar rostrally convex part of the rhinothecae (Figs. 7, 8A-B, 10A/RT). The long beak region was subdivided by the long palatine median ridge rostrally and short papillated line caudally into two halves (right and left) in addition to the median beak nail rostrally (Figs. 7, 9A-B, 11A/MR, MPR, BN). These two rami enclosed the elongated upper mandibular structure named the incomplete

palate that was divided into rostral long beak and the caudal connecting region that demarcated by the slightly oblique transverse ridged (Fig. 7/BP, OP, TBR).

The rostral long beak region is divided into three parts: the rostral ridged part, including the beak nail; the middle smooth part; and the caudal papillary part (Fig. 7/BP, BLP, BSP, BPP). The rostral ridged part was bordered rostrally by the beak nail and medially by the median palatine ridge. In addition, each half contained 3–4 transverse oblique ridges (Fig. 7A-B, 9A-B, 11A/BLP, BN, MR, and RR). The middle smooth part was bordered laterally by the lateral elongated upper mandibular rami and medially by the median palatine ridge (Fig. 7A-B, 9A-B, 11A/BP, MR). The caudal papillary part was bordered laterally by the lateral elongated upper mandibular rami, and medially by the median palatine ridge. Each half had the paramedian papillary ridge and line of the secondary transverse oblique ridges (Fig. 7A, 7C, 9B, 11A/BP, MR, and SRL). The internal surface of the lateral elongated upper mandibular rami carried numerous transverse ridges (Figs. 7A, 7C, 9B, 11A/RLI, RLR), while its external surface was smooth with some folded ridges. The connecting region was divided into choanal and infundibular parts (Figs. 7A, 9A, 12A, 13A/OP, CA, IA). The choanal part consisted of rostral narrow short portion and the caudal wide long part (Figs. 7A, 9A, 12A, 13A/CA, CO, COR, COC).

3.2.3. SEM observations

The upper beak is formed from the two lateral elongated upper mandibular rami and the external semilunar rostrally convex smooth part of the rhinothecae (Fig. 8C, 9D, 10B-D/ERS, RBL, RT). At the area between the end of the short longitudinal ridges and the beginning of the median palatine ridge, there are two aggregations of the small openings of the rostral palatine glands, in which each opening aggregation is located just caudal to the caudal terminal end of each of the two short longitudinal ridges (Fig. 8E-G/red arrowheads, MR, RR). The incomplete palate was divided into rostral long beak and caudal connecting regions. The rostral

long beak region is subdivided into three parts: the rostral ridged part, including the beak nail; the middle smooth part; and the caudal papillary part. The beak nail was bordered rostrally and laterally by the external semilunar rostrally convex smooth part of the rhinothecae and the median papillary area and the beginning of the ridged lateral area of the beak, and medially by the beginning of the median palatine ridge caudally and 2-4 short longitudinal ridges rostrally (Fig. 8C-E/BN, ERS, PMA, RLI, MR, RR). The middle smooth part was bordered laterally by the lateral ridged area of the inner surface of the lateral elongated upper mandibular rami and divided by the median palatine ridge into two equal halves (Fig. 9D, 10B/RLI, MR). The caudal papillary part was bordered laterally by the lateral ridged area of the lateral elongated upper mandibular rami and medially by the median and paramedian papillary palatine ridges; in addition, there are two aggregations of the openings of the lateral palatine salivary glands at its caudal portions (Fig. 10B-G/RLI, MPR, PPR, red arrowheads). The median papillary area was bordered rostrally by the rostral convex smooth external surface and laterally by the beginning of the lateral ridged area of the external surface of the lateral elongated upper mandibular rami (Fig. 8C, 9B-C/PMA, ERS, RLI). This papillary area contains numerous rostrally directed small papillae.

The lateral elongated upper mandibular ramus had two surfaces; the internal ridged surface and the external smooth surface that was covered by the keratinized layer named the rhinothecae (Fig. 8C, 9D, 10B-D, 11B-C, 11E/RBL, EXL, RLI). The rostral part of the internal ridged surface of the lateral upper mandibular ramus (that joined to the median papillary area) had 20–25 longitudinal or oblique ridges (Fig. 8C, 9B-C/RLI, RLR, PMA). The ridged surface of the lateral upper mandibular ramus (opposite to the middle smooth palatine part) had numerous transverse branched ridges, medially to them there are numerous secondary ridges (Fig. 9D-F, 10B-D/RBL, RLI, RLR, and SRL). Opposite to the rostral part of the caudal papillary palatine part, the ridged surface of the lateral ramus had numerous branched transverse ridged and

medially to them there are numerous transverse papillary lines of the elongated, round, or pointed papillae instead of the secondary ridges (Fig. 10D-F/RLR, SPE, SPR, SPP), while the caudal part of the caudal papillary part, the ridged surface of the lateral ramus had numerous non-branched transverse ridged and medially to them there are numerous rostrally directed oblique palatine ridges that extended to the level of the paramedian papillary line (Fig. 11B-E/RBL, RLR, OPR, PPR). Behind the caudal portion of the rostrally directed oblique palatine ridges, there is an aggregation of numerous small openings of the lateral palatine salivary glands (Fig. 11B, 11E-G/OPR, red arrowheads). The terminal part of the lateral upper mandibular ramus, located adjacent to the transverse palatine ridge, contains numerous transverse oblique palatine folds that disappeared completely in the choanal part (Fig. 12B-C/TBR, PFO).

The connecting region of 4.3 cm in length was divided into two parts; the choanal part of 3.2 cm in length and the infundibular part of 0.8 cm in length, and in between there is a median connecting area of 0.3 cm in length. The choanal part was separated from the caudal papillary part of the oropharyngeal roof by a transverse palatine ridge on each side of the rostral beginning of the choana (Fig. 12B-C/TBR, COR). The choanal part had an elongated median opening that divided into two rostral narrow short portion and caudal wide long parts. This median opening divided the choanal part into right and left equal halves (Fig. 12B-C, 12E, 13B-C/CA, CO, COR, COC). The rostral narrow short choanal portion was subdivided into the rostral non-papillated part that was bordered by a smooth border and the caudal papillated part that was bordered by a single papillary row of numerous small short caudomedially directed papillae on each side (Fig. 12B-C/COR, CRP, green arrowheads).

The caudal wide long choanal part was bordered on each side by three papillary rows: the inner first papillary row had numerous medially directed triangular pointed papillae, the middle second papillary row had large and small conical caudolaterally directed papillae, and the outer

third papillary row had numerous long triangular pointed caudolaterally directed papillae (Fig. 12B, 12E, 13B-C/COC, CPF, CPS, and CPT). With high magnification, the papillary surface is visible, and in between are numerous small papillary scales (Fig. 12F/CPS). Each choanal half was subdivided into rostral short smooth, middle short papillary, and long caudal glandular parts (Fig. 12B-C, 12E, 13B-C/RCP, MCP, CCP). The rostral smooth part was opposite to the rostral narrow choanal part, just caudal to the transverse palatine ridge to the filiform papillary aggregation, and it had a small number of palatine salivary gland openings, scales, and tubercles (Fig. 12B-D/RCP, COR, TBR, FIP, red arrowheads, COS, COT). The middle short papillary part (nearly at the beginning of the long wide choanal part) had filiform papillary aggregation in the form of two oblique transverse rows of caudally directed pointed papillae that carried numerous papillary scales with magnification (Fig. 12B, 13E/MCP, FIP). The long caudal glandular part was located between the filiform papillary aggregation and the terminal end of the wide long choanal part, in addition to the presence of numerous oval salivary gland openings (Fig. 12B, 12E-F, and 13B-D/CCP, red arrowheads).

The infundibular part was divided into two halves by the median short depressed groove rostrally and the median narrow short opening, named the infundibular opening (pharyngeal opening of the auditory tube), that connected the pharyngeal cavity with the middle ear and was bordered by an elevated non-papillated ridge (Fig. 13E-F/IA, IF, ICG, FF). Each half of the infundibular part had numerous small, caudally directed, small round openings of the sphenopterygoid salivary glands (Fig. 13E-G/FP, blue arrowheads). With high magnification, the papillary surface is visible, and in between are numerous small papillary scales (Fig. 13G).

3.2.4. SEM morphometric analysis of the different beak processes

In the papillae surrounding the choana, the longest papillary type is the papillae of second (middle) row then the papillae of third (lateral) row, but the shortest ones are the papillae

surrounding the caudal portion of the rostral choanal part, while the widest papillae are the papillae of the second (middle) row then the papillae of third (lateral) row (Table 4). In the palatine region (except the papillae surrounding the choana), the longest and widest papillary type is the filiform papillae in the middle area of the choanal region then the papillae of the papillary border around the choanal part (Table 4). In the rostral portion of the upper and lower beak, there are two regions; the upper papillary region and the lower median papillary teeth-like region. Morphometrically, the lower median papillary teeth-like region is the longest and widest than the upper papillary region (Table 4).

4. DISCUSSION

This study represents the first gross and SEM depictions of the oropharyngeal cavity roof and beak of *A. crecca* duck, and the influence of dietary habits, readily available nutrient components, and environmental, migratory, and climatic factors on the morphological adaptation. The morphological knowledge of the beak and oropharyngeal cavity roof of ducks, particularly *A. crecca*, is limited, with only a few recent articles providing insights into the beak, incomplete palate, and infundibular region (Abumandour et al., 2019; Abumandour and El-Bakary, 2017; Bassuoni et al., 2022).

The beak plays a crucial role in collecting and processing food particles, as described in food intake feeding behavior in avian species, alongside the tongue (Kooloos et al., 1989). The beaks of *Anas platyrhynchos* and *Aythya fuligula* (Kooloos et al., 1989) are similar to our description of the beak and its elongated lower and upper mandibular rami, as well as its adaptation to the lingual shape of *A. crecca*. Functionally, the *Anatidae* family's round lingual apex and nail, as well as the beak's teeth, nail, and papillary area, play an important role in the pecking process to grab food particles from the aquatic area because the lingual and beak nails act as a spoon apparatus for the elevations of the caught food particles (Abumandour et al., 2019). Anseriformes' beaks, similar to those of ducks and geese, are crucial for feeding and collecting

food particles from the ground, water, or while drinking (Kooloos et al., 1989). Their beaks play two roles in filter feeding mechanisms: seizing, based on the small space between lamellae, and inertial impact deposition, influenced by beak lamellae and palatine ridges on the oropharyngeal cavity roof, as seen in *A. clypeata, A. platyrhynchos,* and *A. fuligula* (Kooloos et al., 1989). This study confirmed that two filter feeding mechanisms occurr in *A. crecca*. The inertial impact deposition technique that mainly occurs on the different palatine ridges on the oropharyngeal cavity roof, including the median and paramedian palatine ridges rostrally, the median and paramedian papillary palatine ridges, and the oblique and transverse palatine ridges caudally. The seizing technique is performed by the serrated external surface of the lateral lower beak ramus in the presence of four types of laterally projected processes (oblique long transverse, wedge-like projected, cap-like, and serrated border-like), in addition to the internal serrated ridged surface of the upper beak in the presence of numerous oblique ridges, transverse ridges, secondary ridges, and secondary papillary palatine ridges.

Our study demonstrated that the beak possesses specialized adapted features that have not been previously reported in other avian species, including the *Anatidae*. *A. crecca* lower beak has unique adaptations for dietary specialization due to its serrated external surface of the beak ramus. It is divided into three distinct regions based on processes: rostral, middle, and caudal. The rostral region has two types of oblique long transverse and wedged-like projected processes, the middle region has oblique long transverse and cap-like processes, and the caudal region has slightly oblique transverse and serrated border-like processes. The upper beak's internal serrated surface is divided into three parts: the beak nail, rostral ridged surfaces with longitudinal or oblique ridges, the middle part with numerous transverse branched ridges, and the caudal papillary part. The rostral part has numerous branched transverse ridges, and medially to them is transverse papillary lines of elongated, round, or pointed papillae, while the caudal part has numerous non-branched transverse ridges, and medially to them are

numerous rostrally directed oblique palatine ridges. Functionally, our study confirmed that upper beak lamellae on the internal surface of food particles aid in their filtration process from water (Kooloos et al., 1989). Moreover, this study described the migratory behavior of *A. crecca*'s elongated flat beak with a round rostral border, lower teeth-like region, and upper papillary region to adapt to the feeding filtering pattern. The findings revealed a lower serrated external lateral surface and an upper internal serrated surface, similar to the garganey described by Abumandour et al. (2019). On the other hand, Sayed et al. (2019) observed that there are transverse furrows, giving the lateral edge of the turkey beak a serrated appearance. Numerous avian species, including the hoopoe, Egyptian nightjar, Eurasian collared dove, and hooded crow, exhibit smooth, thin, and sharp lateral and median beak edges (Abumandour and Gewaily, 2019; El-Mansi et al., 2020; El-Mansi et al., 2021; Gewaily and Abumandour, 2020). The choanal part of the beak of *A. crecca* is separated from the caudal papillary part by the transverse palatine ridge, similar to the findings in garganey, *A. platyrhynchos*, and *A. fuligula* (Abumandour et al., 2019; Kooloos et al., 1989). The elongated median choana is divided into a rostral short part and a caudal wide long part, similar to species like the coot, hobby, sparrow, dove, pigeon, African pied crow, *A. platyrhynchos*, and *A. fuligula* (Abumandour, 2014, 2018; Abumandour et al., 2019; Abumandour and El-Bakary, 2017; Abumandour et al., 2021a; El-Mansi et al., 2021; Igwebuike and Eze, 2010; Kooloos et al., 1989). In contrast, in southern lapwings (Erdoğan and Pérez, 2015), the rostral part of the choanal cleft is a longer and wider part. The choana in the Egyptian nightjar has a similar width, except for its wide cranial portion (El-Mansi et al., 2020).

There are species-specific variations in the papillation of the choana among the different birds. Our study provides a unique description of the choana that has not previously been described, in which the rostral narrow choana is subdivided into the rostral non-papillated part and the caudal papillated part with a single papillary row, while the caudal long wide papillated part

has three papillary rows on each side: the inner row of numerous medially directed triangular papillae, the middle row of large and small conical caudolaterally directed papillae, and the outer row of numerous long triangular caudolaterally directed papillae. Meanwhile, there is one papillary row surrounding the rostral part and two papillary rows surrounding the caudal part of the choana in *A. platyrhynchos*, *A. fuligula,* and *A. clypeata* (Kooloos et al., 1989), while there are two papillary rows completely surrounding the choana in the sparrow and moorhen (Abumandour, 2018; Bassuoni et al., 2022), while the choana is described as a non-papillary opening in the Egyptian nightjar (El-Mansi et al., 2020). However, there is a single papillary row surrounding the rostral part of the choana in the coot (Abumandour and El-Bakary, 2017), and two papillary rows surrounding the rostral part of the choana in the Eurasian collared dove (El-Mansi et al., 2021), while there are two papillary rows surrounding the caudal part of the choana only in the garganey (Abumandour et al., 2019). The findings of this study align with previous studies showing that a caudally or caudomedially directed papillary row prevents food particles from entering the choanal cleft (Abumandour et al., 2019; Bassuoni et al., 2022). Moreover, our study identified a distinct choanal half of the choanal field, divided into three areas: rostral short smooth, middle short papillary, and long caudal glandular. The middle papillary part has filiform aggregations in the form of two oblique transverse rows, while the long glandular part has numerous oval laryngeal salivary gland openings.

The infundibulum area is neglected in previously published articles on all duck species, except that described in garganey (Abumandour et al., 2019) and some recently published articles on other birds (Abumandour, 2018; Abumandour and El-Bakary, 2017; Abumandour et al., 2021a; Abumandour and Gewaily, 2019; Abumandour et al., 2021b; Bassuoni et al., 2022; El-Mansi et al., 2020; El-Mansi et al., 2021; Gewaily and Abumandour, 2020). The current study revealed that the infundibular part is divided into two equal halves by a median groove and opening, each with numerous small caudally directed papillae and small round laryngeal

salivary gland openings. The non-papillated infundibular opening described here is similar to that seen in the garganey, hoopoe, Eurasian collared dove, and ostrich (Abumandour et al., 2019; Abumandour and Gewaily, 2019; El-Mansi et al., 2021; Gussekloo and Bout, 2005). However, as shown in the sparrow, coot, and hooded crow, the infundibular aperture is entirely surrounded by numerous caudomedially oriented papillae (Abumandour, 2018; Abumandour and El-Bakary, 2017; Gewaily and Abumandour, 2020), whilst this opening is entirely encircled by only four small papillae in the Egyptian nightjar (El-Mansi et al., 2020).

Previous research indicated significant variation in palatine ridge number and configuration among avian species, suggesting their suitability for different food habits. Our study revealed that the oropharyngeal cavity roof has ten ridges, including two rostral peripheral ridges, a median longitudinal ridge, a single median and two paramedian papillary ridges, two transverse palatine ridges, and two transverse papillary rows on the choanal field, while the oropharyngeal cavity roof floor has only one median longitudinal ridge. The oropharyngeal cavity roof of *A. platyrhynchos, A. fuligula,* and *A. clypeata* contains a median longitudinal, a median paramedian papillary, and two transverse palatine ridges (Kooloos et al., 1989). However (Abumandour et al., 2021b), in the five different post-hatching age stages of the quail, there are twelve palatine ridges; eight longitudinal ridges (seven non-papillated and one papillated median ridge), one oblique row, and three transverse papillary rows. Meanwhile, the five papillary rows (four longitudinal rows and one transverse row) were seen in the garganey (Abumandour et al., 2019), Eurasian Hobby (Abumandour, 2014), and Egyptian Nightjar (El-Mansi et al., 2020). Four ridges were observed in the pigeon (Abumandour et al., 2021a), the three ridges in the coot, the Eurasian collared dove, the moorhen, and the pigeon (Abumandour and El-Bakary, 2017; Bassuoni et al., 2022; El-Mansi et al., 2021; Mahdy, 2020). It is noteworthy that the common raven and European magpie have been described as completely devoid of palatine ridges (Erdogan and Alan, 2012). The present work agrees with previous

reports demonstrating that the caudally directed palatine papillae were arranged in rows or randomly distributed (Abumandour, 2018; Abumandour and El-Bakary, 2017), whereas these papillae were completely absent in rock pigeons (Abumandour et al., 2021a).

A characteristic description of the oropharyngeal cavity roof (incomplete palate) that was not previously described is introduced in this study. The oropharyngeal cavity roof, a crucial part of the feeding system, is seldom discussed in literature, except in three duck species by Kooloos et al (1989). Our study identified the oropharyngeal cavity roof as an elongated upper mandible surrounded by a smooth, hard, keratinized structure called the rhinothecae, similar to that described in *A. platyrhynchos* and *A. fuligula* (Kooloos et al., 1989). The current study added that the upper mandible had two laterally elongated mandibular rami that communicated rostrally with the semilunar rostrally convex part of the rhinothecae. In addition, the oropharyngeal cavity roof is divided into two major regions, the rostral long beak and the caudal connecting region, marked by a slightly oblique transverse ridge. The long beak region is subdivided into three parts, the rostral ridged the middle smooth, and the caudal papillary part, while the connecting region is divided into choanal and infundibular parts. Moreover, the internal surface of the lateral elongated upper mandibular rami carried numerous transverse ridges, while its external surface was smooth with some folded ridges. The slightly oblique transverse ridge, choana, and infundibulum area were described previously in *A. platyrhynchos* and *A. fuligula* (Kooloos et al., 1989). Furthermore, the current findings provided the first description of two distinct regions in the rostral part of the oropharyngeal cavity roof and floor. The upper median papillary region carries numerous small papillae and the lower semilunar teeth-like papillary region possesses numerous teeth-like papillae. The lower semilunar teeth-like papillary region has a median-situated teeth-like papilla with a deep space, surrounded by a circular border and filiform-like papillae, while the periphery-situated teeth-like region was oblique rostrally triangular with a shallow space and an incomplete caudally border. The

papillary system of the oropharyngeal cavity roof of the examined *A. crecca* exhibited two appearances. The first appearance is the papillary ridges such as the median papillary area (possessed numerous rostrally directed small papillae on the rostral tip of the lower beak), median and two paramedian papillary palatine ridges (on the middle part of the roof), three longitudinal papillary rows surrounded the choana, two filiform papillary rows on the middle part of the choanal field, and the papillary border surrounded the choana. The second appearance is the randomly distributed round and elongated papillae (around the region of the median papillary palatine ridge) and the numerous caudally directed papillae on the infundibular area.

5. CONCLUSION

Our study is the first morphological effort to characterize the beak and palatine adaptations with their species-specific feeding behaviors, to identify the feeding sieving technique in *A. crecca*. In terms of food particle capture, the lower median papillary teeth-like region corresponded to the lower papillary region. The serrated gnathotheca surface had transverse, wedge-like, cap-like, and serrated border-like processes. The rostral long beak region had the rostral ridged part with its nail, the middle, and the caudal papillary part. The rostral choanal part had a rostral non-papillated and a caudal papillated part, while the caudal choanal papillated part was bordered by three papillary rows. The infundibular plate had numerous papillae and sphenopterygoid salivary gland openings. Consequently, beak and palate structures exhibit anatomical adaptations for efficiently filtering feeding mechanisms.

Authors contribution

Conceptualization: M.A.A., D.M., M.K., A.A.E., and A.M.M.; Methodology: M.A.A., R.S.A., F.F., H.H., D.M., M.K., A.A.E., and A.M.M.; Investigation: M.A.A., R.S.A., F.F., H.H., D.M., M.K., A.A.E., and A.M.M.; Data analysis: M.A.A., F.F., D.M., and H.H.; Resources: R.S.A.,

M.A.A., and F.F.; Writing-Original draft: M.A.A., R.S.A., F.F., H.H., D.M., M.K., and A.A.E.; Writing-Review and editing: A.M.M.; Funding acquisition: R.S.A. All authors agreed to the submission of the final version of the manuscript.

Conflict of interest

The authors declare no conflicts of interest.

Ethics declarations

This study was carried out according to the Institutional Animal Care and Use Committee (IACUC) protocols of Laboratory Animals, Faculty of Veterinary Medicine, Alexandria University (Approval no.: 11/3/2023/232).

Availability of data and material

The manuscript contains all data supporting the reported results.

Acknowledgments

References:
Abumandour, 2014. Gross Anatomical Studies of the Oropharyngeal Cavity in Eurasian Hobby (Falconinae: Falco Subbuteo, Linnaeus 1758). J Life Sci Res 1, 80-92.
Abumandour, 2018. Surface ultrastructural (SEM) characteristics of oropharyngeal cavity of house sparrow (Passer domesticus). Anat Sci Int 93, 384-393.
Abumandour, Bassuoni, N.F., Hanafy, B.G., 2019. Surface ultrastructural descriptions of the oropharyngeal cavity of Anas querquedula. Microscopy Research and Technique 82, 1359-1371.
Abumandour, El-Bakary, N.E.R., 2017. Morphological Characteristics of the Oropharyngeal Cavity (Tongue, Palate and Laryngeal Entrance) in the Eurasian Coot (Fulica atra, Linnaeus, 1758). Anat Histol Embryol 46, 347-358.
Abumandour, El-Bakary, N.E., Elbealy, E.R., El-Kott, A., Morsy, K., Haddad, S.S., Madkour, N., Kandyel, R.M., 2021a. Ultrastructural and histological descriptions of the oropharyngeal cavity of the rock pigeon Columba livia dakhlae with special refer to its adaptive dietary adaptations. Microscopy Research and Technique 84, 3116-3127.

Abumandour, Gewaily, M.S., 2018. Gross morphological and ultrastructural characterization of the oropharyngeal cavity of the Eurasian hoopoe captured from Egypt. Anatomical Science International.

Abumandour, Gewaily, M.S., 2019. Gross morphological and ultrastructural characterization of the oropharyngeal cavity of the Eurasian hoopoe captured from Egypt. Anat Sci Int 94, 172-179.

Abumandour, Kandyel, R.M., 2020. Age-related ultrastructural features of the tongue of the rock pigeon Columba livia dakhlae in different three age stages (young, mature, and adult) captured from Egypt. Microscopy Research and Technique 83, 118–132.

Abumandour, Shukry, M., Lashen, S., Kassab, M., Kandyle, R., Gewaily, M., El-Mansi, A., El Askary, A., Hamoda, H., Farrag, F., 2021b. Posthatching ultrastructural development of the oropharyngeal cavity roof in five age-stages of Coturnix coturnix (Linnaeus, 1758). Microscopy Research and Technique 85, 71-91.

Bassuoni, N.F., Abumandour, M.M.A., Morsy, K., Hanafy, B.G., 2022. Ultrastructural adaptation of the oropharyngeal cavity of the Eurasian common moorhen (Gallinula chloropus chloropus): Specific adaptive dietary implications. Microscopy research and technique 85, 1915–1925.

Baussart, S., Bels, V., 2011. Tropical hornbills (Aceros cassidix, Aceros undulatus, and Buceros hydrocorax) use ballistic transport to feed with their large beaks. Journal of Experimental Zoology Part A: Ecological Genetics 315, 72-83.

Bels, V., Baussart, S.J.F.i.d.v.f.s.t.b.W.C.P., UK p, 2006. Feeding behaviour and mechanisms in domestic birds. 33-50.

BirdLife International, 2020. Anas crecca. The IUCN Red List of Threatened Species 2020: e.T22680321A181692388. https://dx.doi.org/10.2305/IUCN.UK.2020-3.RLTS.T22680321A181692388.en.

Dimech, M., Stamatopoulos, C., El-Haweet, A.E., Lefkaditou, E., Mahmoud, H.H., Kallianiotis, A., Karlou-Riga, C., 2012. Sampling protocol for the pilot collection of catch, effort and biological data in Egypt. Food and Agriculture Organization of the United Nations. https://www.fao.org/ publi catio ns/card/en/c/2f11c e49-f36a-5f43-8f66-d77b2 388d8 93/. EastMed Technical Documents.

El-Mansi, Al-Kahtani, M., Abumandour, M., Ezzat, A., El-Badry, D., 2020. Gross anatomical and ultrastructural characterization of the oropharyngeal cavity of the Egyptian nightjar Caprimulgus aegyptius: Functional dietary implications. Ornithological Science 19, 145-158.

El-Mansi, El-Bealy, E.A., Al-Kahtani, M.A., Al-Zailaie, K.A., Rady, A.M., Abumandour, M.A., El-Badry, D.A., 2021. Biological Aspects of the Tongue and Oropharyngeal Cavity of the Eurasian Collared Dove (Streptopelia decaocto, Columbiformes, Columbidae): Anatomical, Histochemical, and Ultrastructure Study. Microscopy and Microanalysis 27, 1234-1250.

Erdogan, S., Alan, A., 2012. Gross anatomical and scanning electron microscopic studies of the oropharyngeal cavity in the European magpie (Pica pica) and the common raven (Corvus corax). Microsc Res Tech 75, 379–387.

Erdoğan, S., Pérez, W.J.A.Z., 2015. Anatomical and scanning electron microscopic characteristics of the oropharyngeal cavity (tongue, palate and laryngeal entrance) in the southern lapwing (Charadriidae: Vanellus chilensis, Molina 1782). 96, 264-272.

Gewaily, M.S., Abumandour, M.M., 2020. Gross morphological, histological and scanning electron specifications of the oropharyngeal cavity of the hooded crow (Corvus cornix pallescens). Anatomia, histologia, embryologia 50, 72-83.

Gussekloo, S.W.S., Bout, G.R., 2005. The kinematics of feeding and drinking in palaeognathous birds in relation to cranial morphology. J. Exp. Biol. 208, 3395-3407.

Igwebuike, U.M., Eze, U.U.J.V.a., 2010. Anatomy of the oropharynx and tongue of the African pied crow (Corvus albus). 80, 523-531.

Jackowiak, H., Skieresz-Szewczyk, K., Godynicki, S., Iwasaki, S.i., Meyer, W., 2011. Functional morphology of the tongue in the domestic goose (Anser anser f. domestica). Anat Rec 294, 1574-1584.

King, A.S., McLelland, J., 1984. Birds, their structure and function. Bailliere Tindall, 1 St. Annes Road.

Kooloos, J., Kraaijeveld, A., Langenbach, G., Zweers, G.J.Z., 1989. Comparative mechanics of filter feeding in Anas platyrhynchos, Anas clypeata and Aythya fuligula (Aves, Anseriformes). 108, 269-290.

Madge, S., Burn, H., 1988. Wildfowl: an identification guide to the ducks, geese and swans of the world. A&C Black.

Mahdy, M.A.A., 2020. Comparative gross and scanning electron microscopical study of the oropharyngeal roof of young and adult domestic pigeon (Columba livia domestica). Microsc Res Tech 83, 1045-1055.

Nickel, R., schummer, A., Seiferle, E., 1977. Anatomy of the Domestic Birds. Translation by W.G.Siller and P.A.L.Wight. Verlag Paul Parey, Berlin. Hamburg.

Roshdy, K., Morsy, K., Abumandour, M.M., 2021. Microscopic focus on ependymal cells of the spinal cord of the one-humped camel (Camelus dromedarius): Histological, immunohistochemical, and transmission microscopic study. Microscopy Research and Technique 85, 1238-1247.

Sayed, A.E.D.H., Mahmoud, U.M., Essa, F., 2019. The microstructure of buccal cavity and alimentary canal of Siganus rivulatus: Scanning electron microscope study. Microscopy research and technique 82, 443-451.

Schwenk, K., Rubega, M., 2005. Diversity of vertebrate feeding systems. Physiological and ecological adaptations to feeding in vertebrates, 1-41.

Tadjalli, M., Mansouri, S.H., Poostpasand, A., 2008. Gross anatomy of the oropharyngeal cavity in the ostrich (Struthio camelus). Iranian J Vet Res 9, 316-323.

Tomlinson, B.C.A., 2000. Feeding in paleognathous birds. In: Feeding: Form, Function, and Evolution in Tetrapod Vertebrates (K. Schwenk ed). San Diego: Academic Press, pp. 359–394.

Tables:

Table 1. Length and width of the different parts of the oropharyngeal cavity floor of the migratory *A. crecca*.

Parts of the oropharyngeal cavity floor	Length (cm)
Length of rostral part of lower beak that does not occupy by tongue (LBR)	0.5 ± 0.12
Length of the lower beak	5.5 ± 0.35
Length of the lower mandibular ramus (LRB)	5 ± 0.23
Length of the lower mandibular space	5 ± 0.31
Length of lower mandibular space till beginning of lingual frenulum	3.5 ± 0.21
Length of the rostral smooth space (SDR)	0.2 ± 0.03
Length of the middle folded space (FDR)	0.3 ± 0.02
Length of the long sublingual space (SLS)	4 ± 0.3
Length of the caudal sublaryngeal space	0.5 ± 0.02

Table 2. Length and width of the different types of processes of the oropharyngeal cavity floor of the migratory *A. crecca*.

Process	Average length (μm)	Average width (μm)
Transverse processes	1.8 ± 0.34	0.51 ± 0.024
Wedge-like processes	0.45 ± 0.14	0.3 ± 0.04
Cap-like processes	1.01 ± 0.56	1.4 ± 0.32
serrated border-like processes	2.1 ± 0.53	0.4 ± 0.224

Table 3. Length and width of the different parts of the oropharyngeal cavity roof of the migratory *A. crecca*.

Parts of the oropharyngeal cavity floor		Cm
Length of oropharyngeal cavity roof		8 ± 0.8
The rostral long beak of palate	Length	5 ± 0.82
	Length of the rostral ridged part	0.5 ± 0.05
	Length of the beak nail	0.2 ± 0.001
	Length of the middle part	2.8 ± 0.1
	Length of the caudal papillary part	1.5 ± 0.4
Length of the choanal region		2.1 ± 0.4
Choana	Length	1.9 ± 0.3
	Width	0.3 ± 0.001
The rostral narrow choanal part	Length	0.5 ± 0.015
	Length of a rostral non-papillated	0.2 ± 0.013
	Length of caudal papillated part	0.3 ± 0.011
Length of caudal papillated wide choanal part		1.4 ± 0.32
Infundibular region	Length	0.9 ± 0.15
Infundibular opening	Length	0.2 ± 0.012
	Width	0.06 ± 0.004
Length of Median palatine ridge		3.5 ± 0.44
Median palatine papillary ridge		1.5 ± 0.12
paramedian palatine papillary ridge		1.3 ± 0.05
Each half of Transverse palatine ridge		0.5 ± 0.01

Table 4. Length of the different parts of the oropharyngeal cavity roof of the migratory *A. crecca*.

Parts	Length (µm)	Width (µm)
Upper papillary region (RPB)	2 ± 0.05	0.2 ± 0.03
Lower median papillary teeth-like region (RPB)	3 ± 0.5	0.9 ± 0.05
Papillae of caudal portion of rostral choanal part (CRP)	0.1 ± 0.001	0.05 ± 0.001
Papillae of the first row of the caudal choanal part (CPF)	0.6 ± 0.01	0.15 ± 0.01
Papillae of the second row of caudal choanal part (CPS)	0.8 ± 0.02	0.2 ± 0.01
Papillae of the third row of caudal choanal part (CPT)	0.7 ± 0.01	0.17 ± 0.01
Papillae of the filiform papillary aggregation of the middle area of the choanal region (FIP)	0.21 ± 0.02	0.07 ± 0.01
Papillae of papillary border around choanal part (CPR)	0.16 ± 0.02	0.055 ± 0.002

Figures
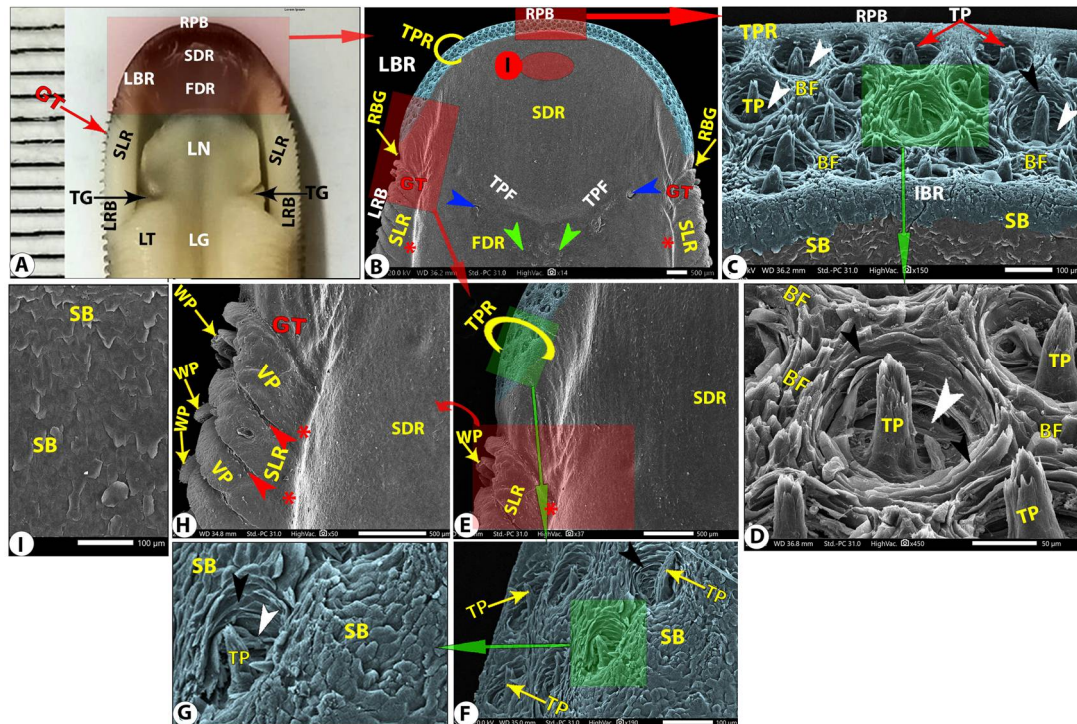
Figure 1. Gross (A) and SEM (B-G) images of the rostral part of the floor of the oropharyngeal cavity of *A. crecca* showing the rostral part of the lower beak (LBR), the semilunar rostrally convex border (RPB), gnathotheca (GT), external serrated surface (SLR) of the lateral lower mandibular ramus (LRB), internal beak ridge (IBR), rostral short smooth space (SDR), folded dorsal surface (FDR), semilunar transverse palatine fold (TPF), shallow longitudinal groove (red asterisk), shallow oblique groove (RBG), the transverse (VP) and wedge-shaped (WP) palatine processes; an oblique shallow groove (red arrowheads), the rostral teeth-like papillary region (TPR) with teeth-like papillae (TP), a depressed round space (white arrowheads), a circular border (black arrowheads), short filiform papillae (BF), beak scales (SB), two large openings of the maxillary salivary glands (blue arrowheads), numerous small openings of the palatine salivary glands (green arrowheads), the median lingual sulcus (LG), the lingual tip (LT), the nail (LN), and the transverse lingual groove (TG).
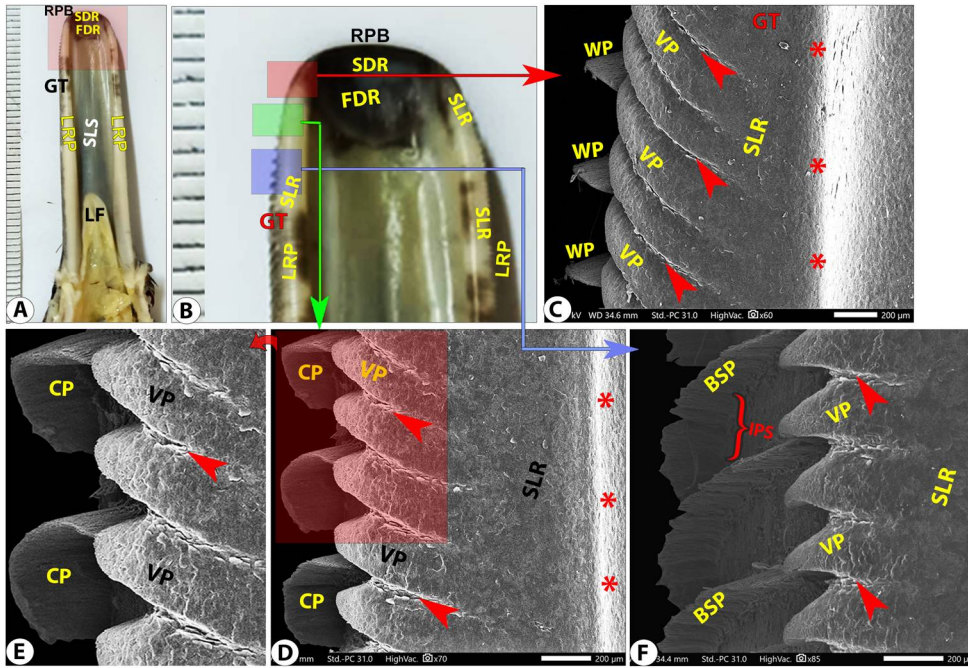
Figure 2. Gross (A-B) images of the lower beak with the removal of the tongue and SEM (C-F) images of the rostral part of the lower beak of *A. crecca* showing the semilunar rostrally convex border (RPB), gnathotheca (GT), external serrated surface (SLR) of the lateral lower mandibular ramus (LRB), rostral short smooth space (SDR), folded dorsal surface (FDR), sublingual space (SLS), the lingual frenulum (LF), shallow longitudinal groove (red asterisk), the transverse (VP), cap-like (CP), serrated border-like (BSP), wedge-shaped (WP) beak processes, oblique shallow groove (red arrowheads), inter-process space (IPS), and rostral teeth-like papillary region (TPR).
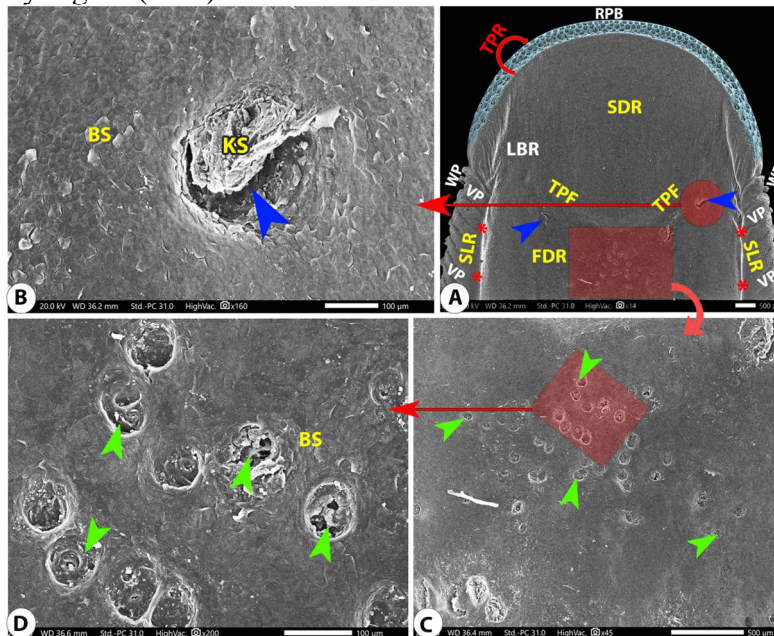
Figure 3. SEM micrographs of the rostral part of the lower mandibular space of the beak of *A. crecca* showing the semilunar rostrally convex border (RPB), external serrated surface (SLR), rostral short smooth space (SDR), folded dorsal surface (FDR), shallow longitudinal groove (red star), semilunar transverse palatine fold (TPF), teeth-like papillary region (TPR), large openings of the maxillary glands (blue arrowheads), keratinized operculum (KS), small openings of the palatine glands (green arrowheads), and beak scales (BS). The transverse (VP) and wedge-shaped (WP) beak processes are clear.
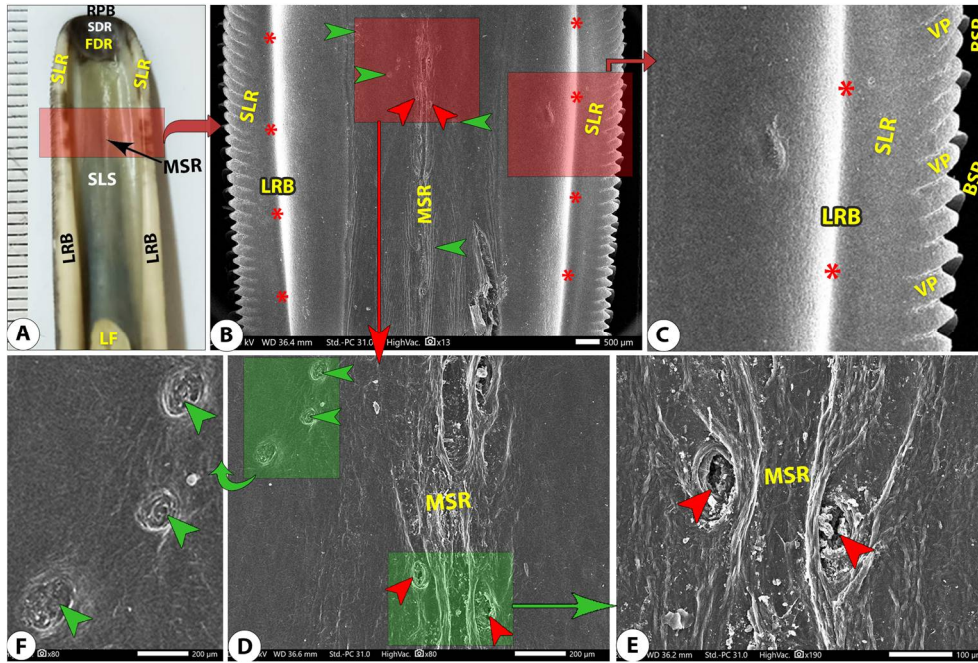
Figure 4. Gross (A) of the lower mandibular beak and SEM (B-F) image of the rostral part of the oropharyngeal cavity floor of *A. crecca* showing the external serrated surface (SLR) of the lateral lower mandibular ramus (LRB), semilunar rostrally convex border (RPB), rostral short smooth space (SDR), folded dorsal surface (FDR), sublingual space (SLS) with the lingual frenulum (LF), shallow longitudinal groove (red star), transverse (VP) and serrated border-shaped (BSP) palatine processes (red arrowheads), shallow sublingual folded ridge (MSR), two large ovoid glandular openings (red arrowheads), and numerous small round openings of the palatine glands (green arrowheads).
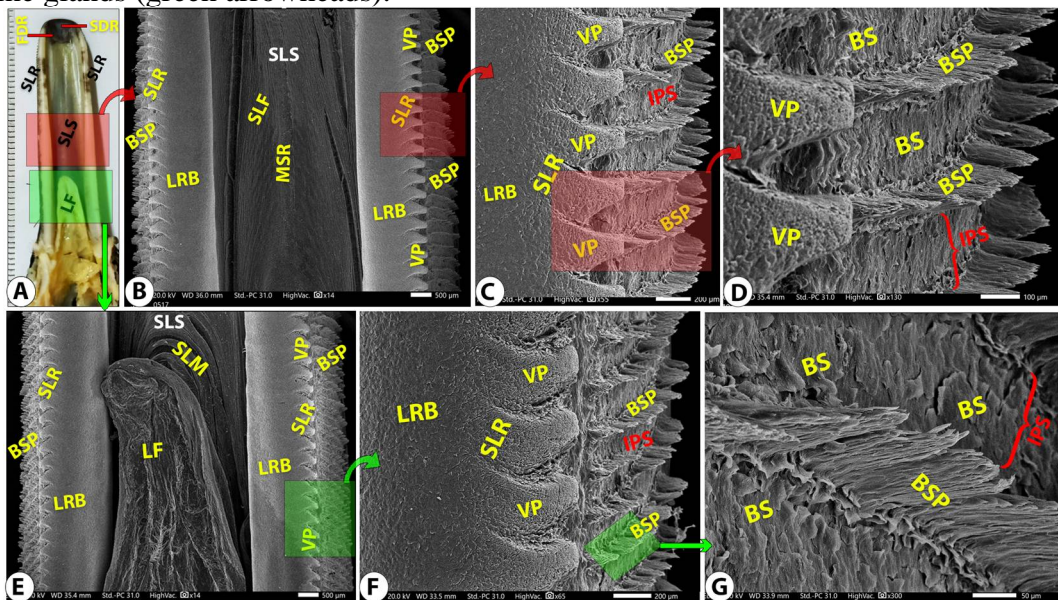
Figure 5. Gross (A) view of the lower mandibular beak and SEM (B-D) images before the level of the lingual frenulum and (E-G) at the level of the lingual frenulum (LF) of the floor of the oropharyngeal cavity of *A. crecca* showing the external serrated surface (SLR) of the lateral lower mandibular ramus (LRB), semilunar rostrally convex border (RPB), rostral short smooth space (SDR), folded dorsal surface (FDR), sublingual space (SLS) with lingual frenulum (LF), longitudinal groove (red star), sublingual muscles (SLM), median sublingual ridge (MSR), transverse (VP) and serrated border-shaped (BSP) palatine processes with scales (BS) inter-process space (IPS).
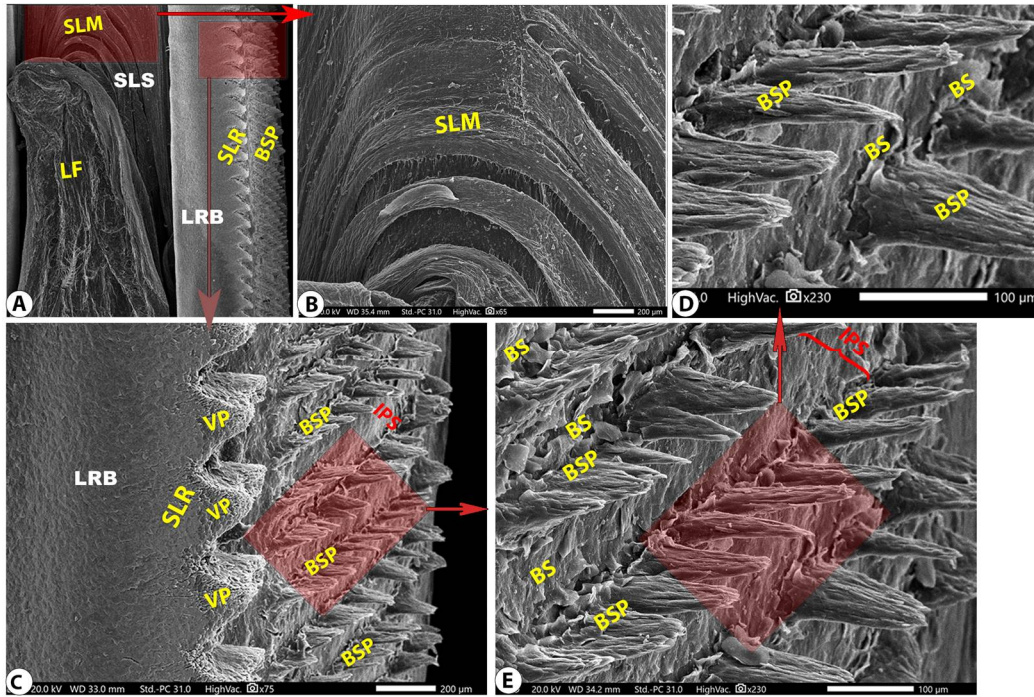
Figure 6. SEM image of the floor of the oropharyngeal cavity of *A. crecca* at the level of the lingual frenulum (LF) showing the sublingual muscles (SLM), the external serrated surface (SLR) of the lateral lower mandibular ramus (LRB) with its transverse (VP) and serrated border-shaped (BSP) palatine processes with scales (BS).
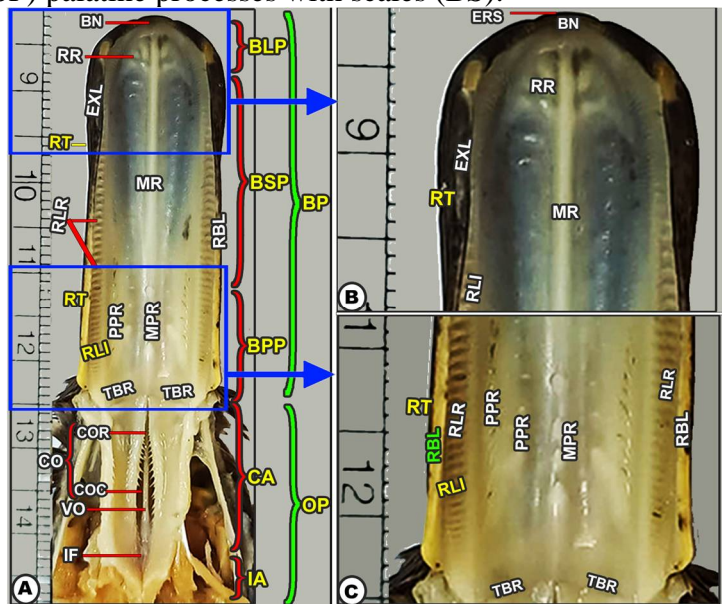

Figure 7. Gross images of the oropharyngeal cavity roof of *A. crecca* (A-C) showing the rhinotheca (RT), the long beak region (BP), which is divided into the rostral part (BLP), the middle part (BSP), and the caudal papillary part (BPP). The smooth external surface (EXL) and inner ridged surface (RLI) with its ridges (RLR), the beak nail (BN) with its rostral convex border (ERS), the lateral mandibular ramus (RBL), the peripheral ridges (RR), the median ridge (MR), the median (MPR), and paramedian papillary (PPR) ridges, the transverse palatine (TBR), and the secondary ridges (SRL). The choanal area (CA) with the choana (CO), which had rostral narrow (COR) and wised caudal (COC) parts, the vomer bone (VO), and the infundibulum area (IA) with the infundibulum (IF).
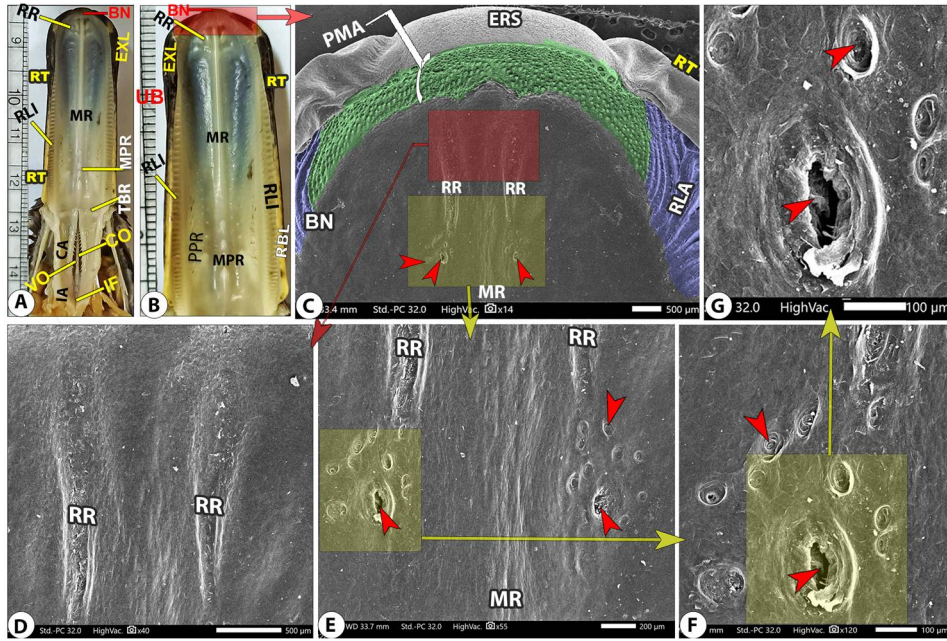
Figure 8. Gross (A-B) and SEM (B-E) images of the oropharyngeal cavity roof of *A. crecca* showing the rhinotheca (RT), the smooth external surface (EXL) and inner ridged surface (RLI) with its transverse (RLR) and oblique (RLA) ridges, beak nail (BN) with its rostral convex border (ERS), lateral mandibular ramus (RBL), peripheral ridges (RR), median ridge (MR), transverse palatine (TBR), median (MPR) and paramedian papillary (PPR) ridges. The connecting region (OP), and the choanal area (CA) with choana (CO) that had rostral narrow (COR) and wised caudal (COC) parts, vomer bone (VO), infundibulum area (IA) with infundibulum (IF), and small openings of the palatine gland (red arrowheads).
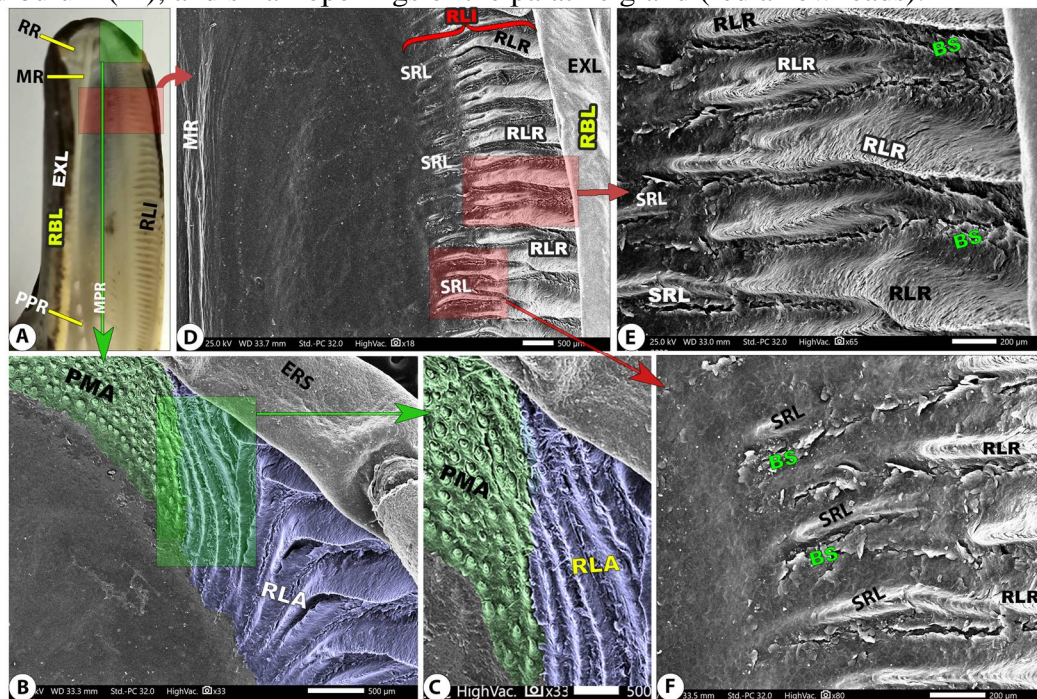

Figure 9. Gross (A) and SEM (B-F) imaged of the rostral part of the oropharyngeal roof of *A. crecca* showing the peripheral (RR) and median (MR), median papillary (MPR), and paramedian papillary (PPR) ridges. The smooth external surface (EXL), inner ridged surface (RLI) with its transverse (RLR), oblique (RLA), and secondary ridges (SRL), rostral convex border (ERS), lateral mandibular ramus (RBL), papillary median region (PMA), and scales (BS).
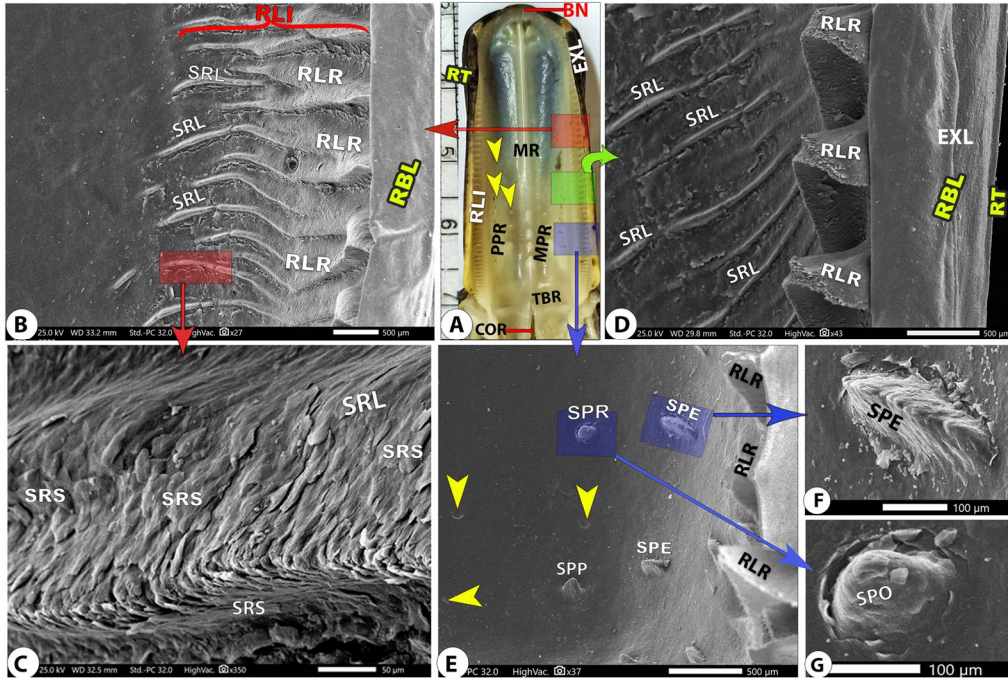
Figure 10. Gross (A) and SEM (B-F) images of the oropharyngeal roof of *A. crecca* showing the rhinotheca (RT), the median palatine (MR), median (MPR), paramedian papillary palatine (PPR), and transverse palatine (TBR) ridges. The smooth external surface (EXL), inner ridged surface (RLI) with its transverse (RLR), secondary ridges (SRL) with its scales (SRS), lateral mandibular ramus (RBL), round (SPR), elongated (SPE), and randomly distributed (yellow arrowheads) papillae.
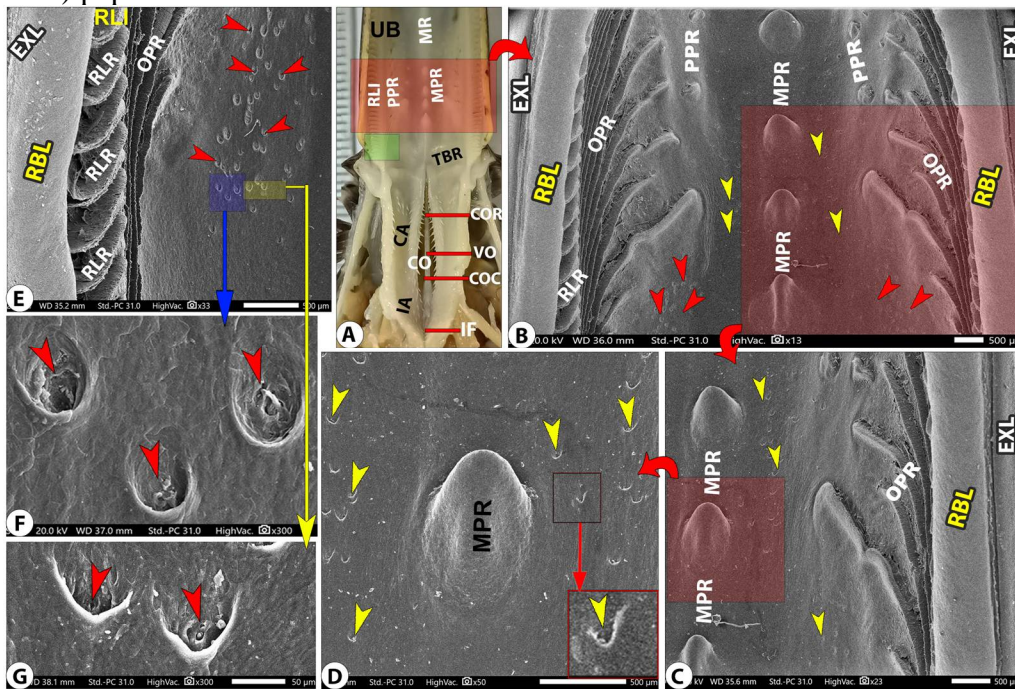

Figure 11. Gross (A) and SEM (B-F) images of the oropharyngeal roof of *A. crecca* showing the median palatine (MR), median (MPR), paramedian papillary palatine (PPR), and transverse palatine (TBR) ridges. The lateral mandibular ramus (RBL), smooth external surface (EXL), inner ridged surface (RLI) with its transverse (RLR), secondary ridges (SRL), oblique palatine ridges (OPR), lateral mandibular ramus (RBL), randomly distributed (yellow arrowheads) papillae, and openings of palatine salivary glands (red arrowheads).
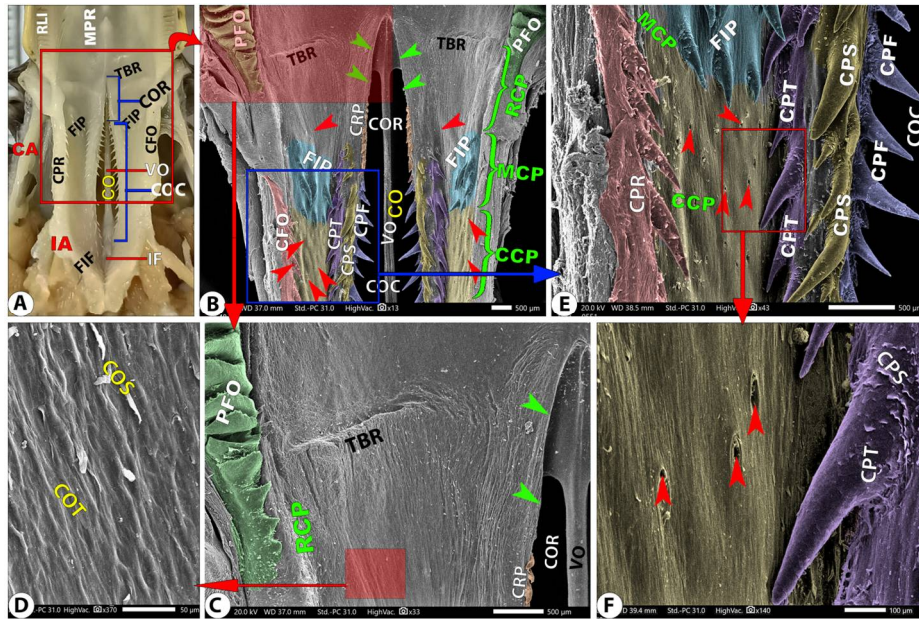
33

Figure 12. Gross (A) and SEM (B-G) images of the caudal part of the pharyngeal cavity roof of *A. crecca* showing the median papillary ridge (MPR), transverse palatine ridge (TBR), and foliate palatine fold (PFO). Each choanal area (CA) had rostral (RCP), the middle papillary (MCP), and the caudal glandular (CCP) part with its surrounded papillary border (CPR), vomer bone (VO), choana (CO) had rostral narrow (COR) with its single papillary row (CRP) and wide caudal parts (COC) with its three papillary rows; inner first (CPF), middle second (CPS), and outer third (CPT) row with papillary scales (CPS). The choanal area had numerous laryngeal salivary gland openings (red arrowheads), a small rostral area of filiform papillae (FIP), scales (COS), and tubercles (COT).
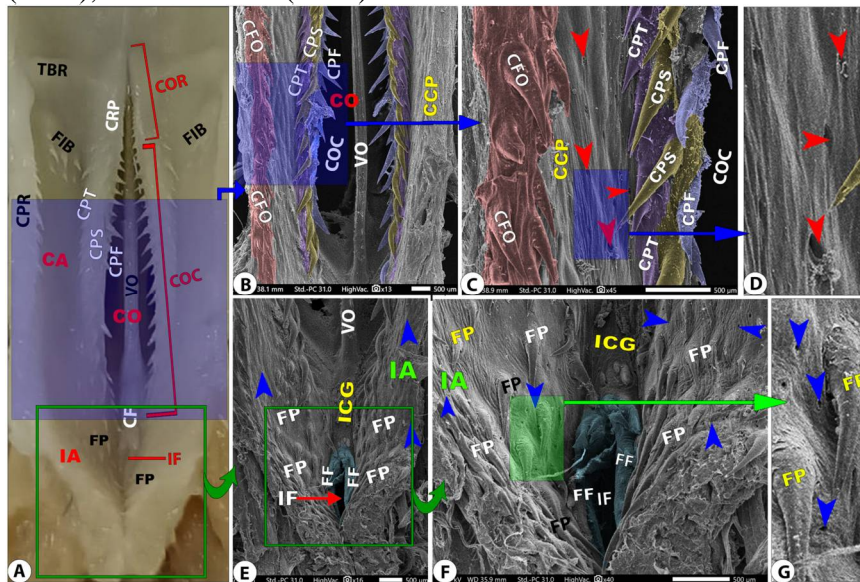

Figure 13. Gross (A) and SEM (B-G) images of the caudal part of the pharyngeal cavity roof of *A. crecca* showing the transverse palatine ridge (TBR), the choanal area (CA) with its surrounded border (CPR), vomer bone (VO), and choana (CO) with its rostral narrow (COR) that had single papillary row (CRP) and wide caudal parts (COC) with its three papillary rows; inner first (CPF), middle second (CPS), and outer third (CPT) row with papillary scales (CPS). The caudal glandular (CCP) part had laryngeal salivary gland openings (red arrowheads) and a rostral area of filiform papillae (FIP). The infundibular area (IA) with its median infundibular groove (ICG) and opening (IF) with its surrounding border (FF), filiform papillae (FP), and sphenopterygoid salivary gland openings (blue arrowheads).

34